Indonesian Journal of Electrical Engineering and Computer Science
Vol. 12, No. 1, October 2018, pp. 246~253
ISSN: 2502-4752, DOI: 10.11591/ijeecs.v12.i1.pp246-253

Faults Signature Extraction in Wind Farm Integrated Transmission Line Topology

Osaji Emmanuel[1], Mohammad Lutfi Othman[2], Hashim Hizam[3], Muhammad M. Othman[4], Elhad Akar. E[5], Okeke Chidiebere. A[6], Nwagbara Samuel .O[7]
[1,2,3,5,6,7]Centre for Advanced Power and Energy Research and Department of Electrical and Electronics Engineering, Faculty of Engineering, Universiti Putra Malaysia, UPM Serdang, Selangor, Malaysia
[4]Centre for Electrical Power Engineering Studies & Faculty of Electrical Engineering, Universiti Teknologi Mara Malaysia, Shah Alam, Selangor, Malaysia

Article Info

Article history:

Received Jun 1, 2018
Revised Jul 10, 2018
Accepted Jul 25, 2018

Keywords:

Renewable green energy sources
entropy energy
unit protection
standard deviation

ABSTRACT

The integration of Renewable Green Energy Sources (RGES) like Wind Farm Generators (WFG), and Photo Voltaic (PV) systems into convention power system as a future solution to the increase in global energy demands, generation cost reduction, and limited climate impact. The innovation introduced protection compromise challenges in power system due to in-feeds fault current penetration from RGES on existing system, leading to an undesired trip of the healthy section of TL, equipment damages, and safety failure. A comparison study of extracted faults signature from two proposed Transmission Line (TL) network topologies with and without WFG integration, for onward fault identification, and classification model design. Descrete wavelet multiresolution Analysis (DWMRA) of extracted one-cycle fault signal signatures from 11 faults type's scenarios in Matlab. Result demonstrated a unique fault signatures across all simulated faults scenarios harness for future work of an adaptive unit protection model for this new area of DG integration.

Corresponding Author:

Osaji Emmanuel,
Centre for Advanced Power and Energy Research and Department of Electrical and Electronics Engineering, Faculty of Engineering,
Universiti Putra Malaysia,
UPM Serdang, Selangor, Malaysia.
Email: osaji.emmanuel@gmail.com

1. INTRODUCTION

The high cost of fossil fuel and global climate changes impact on nonrenewable energy (NRE) sources encouraging the integration of Renewable Green Energy Sources (RGES) on existing power system, considering their environmental friendly, elimination of waste management problem and cost-effectiveness in meeting the ever-increasing electrical energy demands as specified by the Global Wind Energy Council (GWEC) [1]. The integration of Wind Farm Generation (WFG) or Photo Voltaic (PV) RGES sources on existing Transmission Line (TL) network compromises existing protection scheme, leading to wrong trips of the healthy section of the lines and undesired damages to equipment and personnel safety [2]. The increase in WFG sources integrations on existing transmission system have been implemented in countries like the U.S with over 42% installed capacity, Europe, China, and Egypt has installed capacity of 36%. The penetrations introduced some system challenges in term of reliability, security, stability and power quality compromised [3]. The need to provide a more robust protection scheme that is adaptive in nature, towards meeting the current trend of RGES integration as new paradigm is not only necessary but eminent considering the limitations of both existing unit differentia and pilot protection for total TL protection

coverage with high cost of communication channels [4]. Also, the non-unit distance relay protection with partial line protection coverage limitation [5].

Earlier TL protection schemes adopted phasor measurement unit and network system topology information for the protection scheme development for fault identification [6]. An adaptive backup scheme proposed for faulted line and location determination, using limited numbers of the phasor line signals measurements from backup protection zone [7]. Oscillogram data adopted for protection scheme development in high impedance fault detection, using mathematical model and power line communication approach for improved networks safety [8]. Nevertheless, the high computational rigour of these approaches necessitated an improved soft computational intelligent (SCI) approaches for network protection analyses with using advanced digital signal processing (DSP) in combination with Support Vector Machine (SVM) algorithm for ease of computation and accuracy. The cross-country earth fault identification on different TL phases in same circuit using one end signal statistical deviation data for the training of an artificial neuro network (ANN) detection model [9]. In addition, DSP and descrete wavelet transform (DWT) analysis of fault signals waveforms records at monitoring location of a multi-bus meshed network for useful feature information gathering adopted to detect and classify faults [10]. Protection fault analysis scheme on a series and shunt compensated TL on this network topology using half-cycle post-fault current signal for ANN training [11-12]. Other hybrid network topology protection scheme approach for fault identification, classification, and location in combined overhead TL and underground cables network topology using hybrid ANN-Fuzzy logic [13]. The robustness could not be guaranteed due to few numbers of faults scenario simulated in these research work. These reviewed literatures have not presented much works in the new frontier of RGES integration on TL protection scheme development as one challenge and limited to few scenerios studies as motivating factors for this research.

These necessitated the need for the design of a high-speed, low cost and reliable unit protection scheme model development for an integrated WFG-TL protection scheme with detail comparative assessment study of Discrete Wavelet Multiresolution Analysis (DWMRA) of one-cycle during-faults signals (voltage and current) signatures from two TL network topologies with and without WFG integration as case study.

The article organized with the introduction section illustrating the caparative advantages of the RGES against the traditionally existing energy generation sources with respect to cost, environmental assessments effects and negative impacts on existing protections scheme effectiveness. Methodology section divulges the proposed soft computational approach with the application of DWMRA. This is followed by the result and discussion section and finally, the implication of the result expressed in the Conclusion section.

2. RESEARCH METHOD

The CI approach for developing an improve protection classifier model that could be adopted for fault types identification and classificiation in TL protection relay. This will help in preventing and eliminating faults as fast as possible with high precision, selectivity, and reliability

2.1. Propose Unit Protection Classifier Model

This research proposed a Matlab Simulink model of a two-end power generation sources of 132kV, 50Hz, 200 km TL with integrated 9 MW RGES-WFG having six units of 1.5 MW on the common system bus of Figure 1 (a). Simulations scenarios of 11 faults types (AG, BG, CG, ABG, BCG, ACG, ABCG, AB, BC, AC, ABC) where executed across the entire transmission lines at selected fault locations (5, 25, 45, 65, 85, 105, 125, 165, and 185 km), and fault inception angels (0, and 900). The sampling frequency of 50 kHz adopted for one end source fault signal extraction of voltage and currents to eliminate aliasing effect. Figure 2(b) displayed the extracted fault signal samples from phase A single line-to-ground (SLG) fault at 5 km before preprocessing.

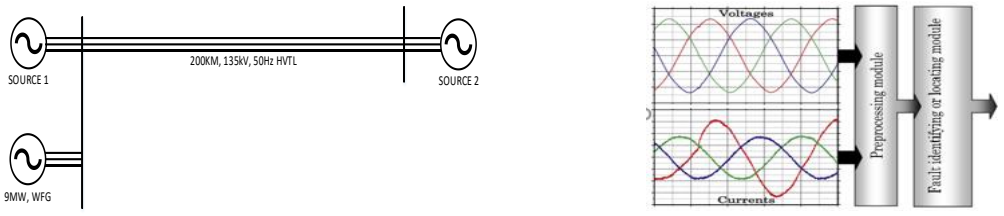

(a) (b)

Figure 1. (a) Integrated WFG-RGES on HVTL (b) Extracted fault voltage and current signals

The signal is preprocessed by passing them through two set cascaded bands filters. The displayed MRA filter architecture of Figure 2 is made up of low pass filter h (k) (LPF) and high pass filters g (k) (HPF) for signal decomposition using DWMRA of extractes one-cycle noisy fault transient signals of voltage and current signatures from two propose networks topologies (with, and without integrated RGES-WFG). The LPF is realised by the scaling function (ϕ) of Equetion 1, the HPF is actualized with the application of the mother wavelet function (Ψ) of Equation 2.

$$\phi(k) = \sqrt{2} \sum_n h(n)\, \phi(2k - n) \tag{1}$$

$$\psi(k) = \sqrt{2} \sum_n g(n)\, \phi(2k - n) \tag{2}$$

Where n is the integer representing the number of samples, k is the translation integer and $\sqrt{2}$ is normalization factor.

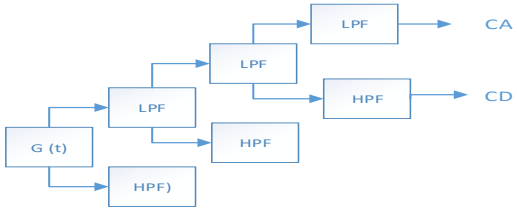

Figure 2. Three level signal decomposition

2.2. DWMRA Application On Fault Signals

WT are small waveforms existing for a short time duration with an average value of zero and mostly adopted in advanced DSP of transient signals study. This is applied in MRA of transient faults signal into translated and scaled components of the applied mother wavelet function studies.The time-frequency localization benefits for little signal disturbances on TL along with the unique ability to extract, and analyze signal signature into various frequencies bands, while retaining the time function information as one of its unique benefits in fault transient studies.The LPF produced the approximate component Aj, while the HPF produces the details Dj component of decomposed signal.These extracted components are adopted for different fault identification and classification scheme of the protective scheme for both proposed TL network topologies. The approximate and detail coefficients relationship between two adjacent levels can be express mathematically by Equation 3 and 4.

$$A_{j+1}(k) = \sum_n h(n - 2k)\, A_j(n) \tag{3}$$

$$D_{j+1}(k) = \sum_n g(n - 2k)\, A_j(n) \tag{4}$$

Where j is the frequency band level. The first stage of the MRA is resolved into two halves of frequency component, while the second stage adopts the LPF output for decomposition into further two halves using another set of LPF and HPF. Subsequent stages further decomposed iteratively till 10th levels of Aj, is attaned using Daubechies (db4) wavelets as the mother wavelet to obtain the fundamental frequency of 50Hz based on a sampling frequency of 50 kHz.

3. RESULTS AND ANALYSIS

The decomposed approximate components of both extracted fault signals at every level of decompositions contain unique signatures based on the signals Standard deviation (STD) and entropy energy content that could be adopted for faults identification, and classification model development. The statistical analysis at 10th level min, max, and STD of the analyzed signal for discriminant application from proposed

network topologies alongsised with the entropy energy contents at the final decomposition level. Figure 3 (a) and (b) display the decomposed voltage comparison study for phase A SLG signatures from propose network topologies. Similar Figure 4 (a) and (b) for fault current signal decomposition. The acronym A, B, C represent phase A, B and While ground involvement in any scenario introduced a capital letter G.

3.1. Ground Fault

Present MRA result of Table 1-10 displayed unique values from both extracted faults signals from proposed network for all possible ground faults based on their min, max, and STD. these uniquesness were harness in the development of ground fault identification model building. The entropy energy and STD values from both signals shows an increase in the current entropy values for SLG faults with RGES-WFG integration as compared to that obtained without integration indicating and infeeding effect from the RGES in Table 1. This is supported by the higher STD values, which reduces with increase in fault distance for both network. Although the STD value is higher for current signal from WFG integrated topology when compared with other topology result in Table 2-4. The decomposed voltage entropy increases, while current the signal entropy reduces with increase in fault distance. Both signals energy contents from integrated WFG network topology are higher compared network without as observe in Table 2-4.

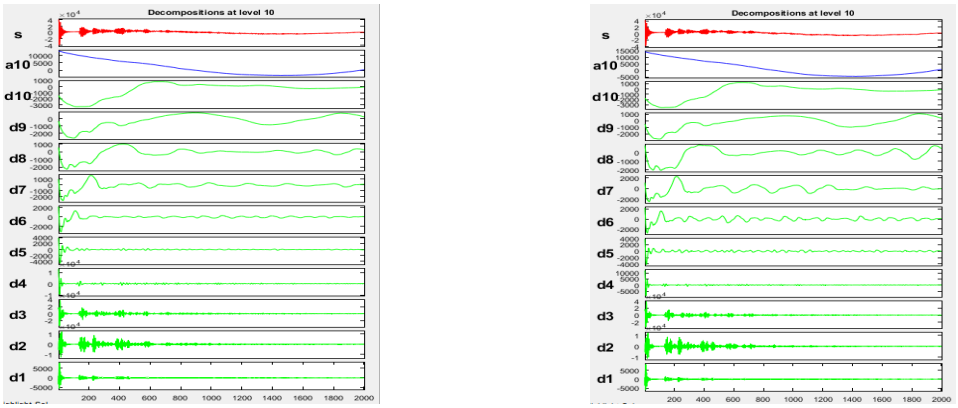

(a) (b)

Figure 3. Voltage signal decomposition (a) without WFG, (b) with WFG integrated PCC

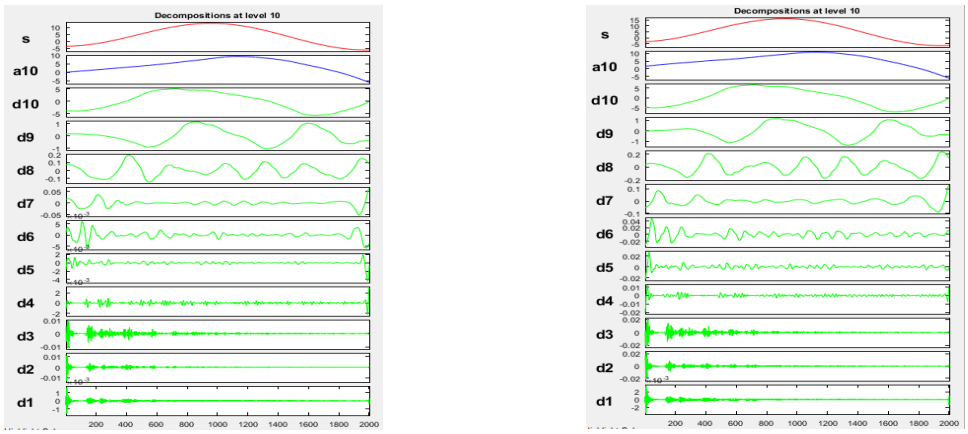

(a) (b)

Figure 4. Current signal decomposition (a) without WFG, (b) with WFG integrated PCC

The obtained result from Doub Line to Ground (DLG) fault for both network recorded much higher STD and entropy energy values from the integrated WFG network for both signals compared to SLG result on Table 5. The three-phase to Ground (ABCG) fault displayed a lower values of STD and entropy energy content for both signasl in Table 6. Furthermore, the entropy energy for DLG faults increases with increase in fault distance for voltage signals but reduces for current signals with increase in fault distance as displayed in Table 7 (a) and 7 (b) respectively. The entropy energy contents obtained from integrated WFG network topology across all DGL is far higher when compared with another network.

Table 1. SLG fault wavelet decomposition result at 5km

Fault Types	Sig.	HVTL STATISTIC WITHOUT WFG Min (-)	Max	STD	Energy	HVTL STATISTICS WITH WFG Min (-)	Max	STD	Energy
Phase	V	3.9311+04	4.0260+04	4632	0.33230+13	3.8040+04	4.1100+04	5220	0.3590+13
AG	I	6.1870	13.0520	6.4310	2.7670+05	6.671	16.0320	7.6940	3.6270+05
Phase	V	8.260+04	7.7720+04	7469	1.4320+13	8.1440+04	7.2680+04	7527	1.4350+13
BG	1	8.4730	9.4410	6.3250	2.3690+05	9.8510	11.2510	7.4370	2.6720+05
Phase	V	3.840+04	4.2780+04	4674	0.3892+13	3.4640+04	4.0780+04	5130	3.6580+13
CG	I	13.0830	3.4100	5.8280	1.4140+05	16.2320	3.2110	6.9450	2.2010+05

Table 2. Phase A-SLG fault across the transmission line

Fault distance	HVTL STATISTIC WITHOUT WFG STD Voltage signal (10^{04})	Current signal	Entropy energy Voltage signal (10^{13})	Current signal (10^{05})	HVTL STATISTICS WITH WFG STD Voltage signal (10^{04})	Current signal	Entropy energy Voltage signal (10^{13})	Current signal (10^{05})
5	0.4632	6.431	0.3323	2.7670	0.5220	7.6940	0.3590	3.6270
25	1.9010	5.5470	0.9295	2.2230	1.8870	6.2540	0.9792	2.6000
45	2.6940	4.9241	1.0930	1.8980	2.6430	5.3260	1.0770	2.0650
65	2.9810	4.4690	1.1080	1.6770	3.1460	4.6900	1.1650	1.7470
85	3.4490	4.1280	1.1670	1.5300	3.4710	4.236	1.2680	1.5430
105	3.8300	3.8650	1.2940	1.4210	3.9350	3.9070	1.3290	1.4060
125	4.0760	3.6620	1.3200	1.3520	4.0190	3.6570	1.3380	1.3220
145	4.4033	3.5010	1.4960	1.2870	4.2540	3.4650	1.4760	1.2560
185	4.7530	3.3020	1.4190	1.2180	4.3800	3.2200	1.4660	1.1590

Table 3. Phase B-SLG fault across the transmission line

Fault distance	HVTL STATISTIC WITHOUT WFG STD Voltage signal (10^{04})	Current signal	Entropy energy Voltage signal (10^{13})	Current signal (10^{05})	HVTL STATISTICS WITH WFG STD Voltage signal (10^{04})	Current signal	Entropy energy Voltage signal (10^{13})	Current signal (10^{05})
5	0.7469	6.3250	1.4320	2.3690	0.7527	7.4370	1.4350	2.6720
25	2.8190	2.8190	3.7640	3.7640	2.3780	6.0060	3.6810	2.1760
45	3.5960	4.8140	4.2050	1.9070	3.0330	5.1050	3.8760	1.9130
65	3.4650	4.3620	4.1600	1.7880	3.4240	4.4950	4.0550	1.7560
85	3.8790	4.0230	4.2310	1.7100	3.6320	4.0610	4.2800	1.6570
105	4.1930	3.7610	4.5170	1.6520	4.1650	3.7470	4.3760	1.5910
125	4.3520	3.5570	4.5090	1.6170	4.1310	3.5050	4.3720	1.5500
145	4.6190	3.3940	4.8520	1.5830	4.3550	3.3200	4.6400	1.5190
185	4.5210	3.1820	4.5210	1.5500	4.3830	3.0790	4.6250	1.4790

Table 4. Phase C-SLG fault across the transmission line

Fault distance	HVTL STATISTIC WITHOUT WFG STD Voltage signal (10^{04})	Current signal	Entropy energy Voltage signal (10^{13})	Current signal (10^{05})	HVTL STATISTICS WITH WFG STD Voltage signal (10^{04})	Current signal	Entropy energy Voltage signal (10^{13})	Current signal (10^{05})
5	0.4674	5.8280	0.3892	1.4140	0.5130	6.9450	3.6580	2.2010
25	1.7460	4.9790	1.0320	1.0320	1.7820	5.5500	0.9691	1.3990
45	2.3800	4.4040	1.1960	0.8011	2.4870	4.6970	1.0960	0.9936
65	2.7070	3.9940	1.2650	0.6567	2.9090	4.1320	0.2909	0.7616
85	3.0780	3.6910	1.3450	0.5578	0.3315	3.7370	1.3220	0.6170
105	3.3650	3.4620	1.4520	0.4882	3.6040	3.6500	1.3940	0.5221
125	3.5880	3.2850	1.5010	0.4374	3.7920	3.2390	1.4450	0.4552
145	3.7690	3.1510	1.5820	0.4024	3.9450	3.0830	1.5070	0.4094
185	3.9940	2.9870	1.6440	0.3675	4.1030	2.900	1.5690	0.3639

Table 5. DLG fault wavelet decomposition result at 5km

Fault Types	Sig.	HVTL STATISTIC WITHOUT WFG Min (-)	Max	STD.	Energy	HVTL STATISTICS WITH WFG Min (-)	Max	STD	Energy
Phase	V	7.5945+04	7.3465+04	5688	0.5081+13	7.4500+04	6.8535+04	6101.5	0.5138+13
ABG	I	7.514	11.2700	6.4570	2.6035+05	7.0125	13.5085	7.001	2.938+05
Phase	V	7.5410+04	7.4325+04	5697.5	0.5217+13	7.3600+04	6.8935+04	6092	0.5251+13
BCG	1	10.8000	6.647	6.1600	1.9125+05	13.0290	6.4195	6.8480	2.377+05
Phase	V	3.9090+04	4.5235+04	5203	0.4750+13	3.652+04	4.8090+04	5557.5	0.4775+13
ACG	I	9.7410	8.3420	6.2440	2.1560+05	10.762	9.0365	6.9070	2.4095+04

Table 6. Three phase-to-ground (ABCG) fault wavelet decomposition result at 5km

Fault Types	Sig	HVTL STATISTIC WITHOUT WFG				HVTL STATISTICS WITH WFG			
		Min (-)	Max	STD	Energy	Min (-)	Max	STD	Energy
ABCG	V	5.435+04	5.4497+04	4340	0.3518+12	5.3003+04	5.3150+04	4198.7	3.5377+12
	I	9.4390	8.8443	6.3413	2.2563+05	9.3597	8.7677	6.3053	2.2207+05

Table 7a. DLG and ABCG fault entropy energy across the TL without WFG integration

Dist	Phase ABG		Phase BCG		Phase ACG		Phase ABCG	
	Signal Enropy energy		Signal entropy energy		Signal entropy energy		Signal entropy energy	
	Voltage (10^{13})	Current (10^{05})	Voltage (10^{13})	Current (10^{05})	Voltage (10^{13})	Current (10^{05})	Voltage (10^{13})	Current (10^{05})
5	0.5081	2.6035	0.5217	1.9125	0.4750	2.1560	0.35177	2.2563
25	2.4400	2.2820	2.4675	1.6445	0.9957	1.9315	1.9536	2.0213
45	2.7885	2.0620	2.7385	1.4825	1.1015	1.6545	2.2030	1.8333
65	2.9690	1.9010	2.8385	1.3559	1.1800	1.4588	2.3260	1.6818
85	3.1135	1.7860	2.9725	1.2693	1.2350	1.3120	2.4557	1.5625
105	3.1235	1.6550	3.0205	1.2074	1.3845	1.1963	2.4873	1.4434
125	3.0465	1.5785	2.8825	1.1490	1.3860	1.1020	2.4113	1.3601
145	3.7940	1.5245	3.3815	1.1038	1.3975	1.0202	2.9717	1.2928
165	3.0890	1.4495	2.9515	1.0678	1.4445	0.9564	2.4973	1.2200
185	3.0875	1.4000	3.0425	1.0381	1.5030	0.8998	2.5390	1.1637

Table 7b. DLG and ABCG entropy energy across the TL with WFG integration

	Phase ABG		Phase BCG		Phase ACG		Phase ABCG	
	Signal Enropy energy		Signal entropy energy		Signal entropy energy		Signal entropy energy	
	Voltage (10^{13})	Current (10^{05})	Voltage (10^{13})	Current (10^{05})	Voltage (10^{13})	Current (10^{05})	Voltage (10^{13})	Current (10^{05})
5	0.5138	2.9380	0.5251	2.3770	0.47745	2.4095	0.3538	2.2207
25	2.2456	2.3460	2.2303	1.7840	0.9972	1.8450	1.7505	1.9820
45	2.3865	2.0445	2.3730	1.5215	1.1325	1.6240	1.8457	1.7893
65	2.5110	1.8525	2.4960	1.3653	1.2030	1.4531	1.9410	1.6360
85	2.5810	1.7125	2.5725	1.2630	1.2130	1.3215	2.0037	1.5100
105	2.6450	1.6100	2.6805	1.1870	1.2700	1.2045	2.0583	1.4088
125	2.7395	1.5305	2.7525	1.1278	1.4175	1.1143	2.1500	1.3250
145	2.7540	1.4620	2.8080	1.0599	1.4475	1.0410	2.1837	1.2517
165	2.7875	1.4100	2.8200	1.0416	1.6020	0.9694	2.2317	1.1927
185	2.9080	1.3655	2.9425	1.0084	1.6975	0.9129	2.3393	1.1405

3.2. Non-Ground Faults

The line to line faults result across both networks topologies indicated an increase in the voltage STD values but decreases for current as the fault distance increses for both proposed network topology in Table 8-11. The STD and entropy values from integrated WFG network topology is lower compared to architecture without integrated WFG. The STD and entropy values remains constant for both ABC and ABCG of Table 11. And Table 7 (a) and (b) respectively.

Table 8. AB Line-line fault analysis result

Fault distance	HVTL STATISTIC WITHOUT WFG				HVTL STATISTICS WITH WFG			
	Standard deviation		Entropy energy		Standard deviation		Entropy energy	
	Voltage (10^{04})	Current	Voltage (10^{13})	Current (10^{05})	Voltage (10^{04})	Current	Voltage (10^{13})	Current (10^{05})
5	2.9545	5.8925	0.9140	2.3530	2.8900	5.9090	0.8866	2.2930
25	4.3180	5.4455	2.6970	2.1510	3.2295	5.4330	2.4665	2.0875
45	5.3765	5.0665	3.0010	1.9900	3.4440	5.0305	2.5600	1.9210
65	5.6155	4.7405	3.1510	1.8615	3.6450	4.6875	2.6525	1.7895
85	5.7540	4.4555	3.2820	1.7670	3.8475	4.3910	2.7010	1.6830
105	5.6825	4.2060	3.2720	1.6490	4.0085	4.1335	2.7400	1.5995
125	5.7615	3.993	3.1695	1.5805	4.1680	3.9070	2.8265	1.5315
145	5.8465	3.7920	3.9045	1.5330	4.2870	3.7085	2.8325	1.4697
165	5.8575	3.6280	3.1835	1.4627	4.3780	3.5310	2.8585	1.4239
185	5.9140	3.4745	3.1740	1.4158	4.4705	3.3715	2.9735	1.3820

Table 9. BC Line-line fault analysis result

Fault distance	HVTL STATISTIC WITHOUT WFG				HVTL STATISTICS WITH WFG			
	Standard deviation		Entropy energy		Standard deviation		Entropy energy	
	Voltage (10^{04})	Current	Voltage (10^{13})	Current (10^{05})	Voltage (10^{04})	Current	Voltage (10^{13})	Current (10^{05})
5	2.9550	5.4135	0.9012	1.5135	2.8965	5.3940	0.8975	1.4995
25	4.3505	4.3505	2.7090	2.7100	3.1920	4.9785	2.4510	1.3940
45	4.9715	4.6795	2.9360	1.3250	3.7280	4.6260	2.5510	1.3065
65	4.9905	4.3870	3.0185	1.2573	3.4890	4.3225	2.6475	1.2361
85	4.9425	4.1320	3.1475	1.2001	3.6255	4.0600	2.7095	1.1788
105	4.7525	3.9075	3.1840	1.1575	3.7355	3.8295	2.7590	1.1314
125	4.6975	3.7085	3.0240	1.1180	3.8445	3.6260	2.8465	1.0917
145	4.6785	3.5315	3.5180	1.0827	3.9320	3.4455	2.8725	1.0581
165	4.6035	3.3730	3.0660	1.0557	4.0145	3.2835	2.9215	1.0289
185	4.5825	3.2300	3.1275	1.0307	4.0980	3.1390	3.0275	1.0044

Table 10. AC Line-line fault analysis result

Fault distance	HVTL STATISTIC WITHOUT WFG				HVTL STATISTICS WITH WFG			
	Standard deviation		Entropy energy		Standard deviation		Entropy energy	
	Voltage (10^{04})	Current	Voltage (10^{13})	Current (10^{05})	Voltage (10^{04})	Current	Voltage (10^{13})	Current (10^{05})
5	2.9210	5.4830	1.3990	1.9886	2.8700	5.5330	1.3540	2.0485
25	2.9785	5.0950	1.4115	1.7645	2.9275	5.1135	1.3660	1.8001
45	3.1125	5.0625	1.4425	1.5872	3.0345	4.7575	1.3890	1.6047
65	3.2930	4.4745	1.4865	1.4437	3.1705	4.4515	1.4180	1.4786
85	3.4990	4.2220	1.5190	1.3273	3.3235	4.1860	1.4520	1.3216
105	3.7030	4.0000	1.5625	1.2196	3.4815	3.9530	1.4885	1.2181
125	3.9195	3.8460	1.6550	1.1399	3.6420	3.7480	1.5245	1.1319
145	4.1355	3.6270	1.6860	1.0713	3.7960	3.5665	1.5685	1.0576
165	4.3465	3.4745	1.7925	1.0045	3.9375	3.4040	1.6025	0.9965
185	4.5585	3.3350	1.8345	0.9496	4.0750	3.2580	1.6275	0.9433

Table 11. Three phase ABC fault analysis result

Fault distance	HVTL STATISTIC WITHOUT WFG				HVTL STATISTICS WITH WFG			
	Standard deviation		Entropy energy		Standard deviation		Entropy energy	
	Voltage (10^{04})	Current	Voltage (10^{13})	Current (10^{05})	Voltage (10^{04})	Current	Voltage (10^{13})	Current (10^{05})
5	0.4340	6.3413	0.3518	2.2563	0.4198	6.3053	0.3538	2.2207
25	3.0013	5.8543	1.9536	2.0213	1.4030	5.8023	1.7505	1.9820
45	3.9047	5.4363	2.2030	1.8333	1.8483	5.3720	1.8457	1.7893
65	4.1273	5.0737	2.3260	1.6818	2.2247	5.0003	1.9410	1.6360
85	4.2747	4.7540	2.4557	1.5625	2.5673	4.6747	2.0037	1.5100
105	4.2593	4.4717	2.4873	1.4434	2.8447	4.3887	2.0583	1.4088
125	4.3873	4.2230	2.4113	1.3601	3.1047	4.1340	2.1500	1.2794
145	4.5367	3.9930	2.9717	1.2928	3.3163	3.9070	2.1837	1.2517
165	4.6253	3.7937	2.4973	1.2200	3.4953	3.7013	2.2317	1.1927
185	4.7583	3.6090	2.5390	1.1637	3.6677	3.5147	2.3393	1.1405

4. CONCLUSION

The individual uniques STD, and entropy energy signature values from the DWMRA of the fault signals across all 11 fault types will be adopted for the fault identification and classifier model building for an adaptive relay protection model building for an improved adaptive system model realization as proposed. The displayed result have help to substantiate the existing uniques in the protection impedances as a result of infeeds contribution into the faulted point from the integrated RGES which compromises the safety system when compared to same network topology without any integrations as demonstrated from the results. The discriminant features exixting between the ground fault and non ground fault analysis can also be adopted to build a fault type classifier model that could distinguish between gonrd and non-ground fault intelligent decision model.This research paper result have demonstrated unique fault signatures across all simulated faults scenarios that will be harness in future work for onward for the building of an adaptive intelligent unit protection relay model in this new area of DG integration protection on TL.The impact assessment study of the infeed effect of integrated RGES-WFG on TL established. Future progress will be achieved by integrating this unique extracted approximate coefficient for an onward building of an adaptive intelligent relay system.

REFERENCES

[1] Paliwal P, Patidar NP, Nema RK. "Planning of grid integrated distributed generators: A review of technology, objectives and techniques". *Renew Sustain Energy Rev*. 2014;40(1):557–70.

[2] Esmaeilian A, Popovic T, Kezunovic M. "Transmission line relay mis-operation detection based on time-synchronized field data". *Electr Power Syst Res*. 2015;125:174–83.

[3] Passey R, Spooner T, MacGill I, Watt M, Syngellakis K. "The potential impacts of grid-connected distributed generation and how to address them: A review of technical and non-technical factors". *Energy Policy*. 2011;39(10):6280–90.

[4] dos Santos A, Barros MTC De, Correia PF. "Transmission line protection systems with aided communication channels—Part II: Comparative performance analysis". *Electr Power Syst Res* 2015;127:339–46.

[5] Hajjar A a. "A high speed noncommunication protection scheme for power transmission lines based on wavelet transform". *Electr Power Syst Res*. 2013;96:194–200.

[6] Neyestanaki MK, Ranjbar a M. "An Adaptive PMU-Based Wide Area Backup Protection Scheme for Power Transmission Lines". *IEEE Trans Smart Grid*. 2015;6(3):1550–9.

[7] Tzu-Chiao L, Pei-Yin L, Chih-Wen L. "An Algorithm for Locating Faults in Three-Terminal Multisection Nonhomogeneous Transmission Lines Using Synchrophasor Measurements". *Smart Grid, IEEE Trans*. 2014;5(1):38–50.

[8] Batista OE, Flauzino RA, De Araujo MA, De Moraes LA, Da Silva IN. "Methodology for information extraction from oscillograms and its application for high-impedance faults analysis". *Int J Electr Power Energy Syst*. 2016;76:23–34.

[9] Swetapadma A, Yadav A. "All shunt fault location including cross-country and evolving faults in transmission lines without fault type classification". *Electr Power Syst Res*. 2015;123:1–12.

[10] J. Lázaro a, J.F. Miñambresb MAZ b, A. "Selective estimation of harmonic components in noisy electrical signals for protective relaying purposes". *Int J Electr Power Energy Syst*. 2014;56(1):140–6.

[11] Vyas B, Das B, Maheshwari RP. "An improved scheme for identifying fault zone in a series compensated transmission line using undecimated wavelet transform and Chebyshev Neural Network". *Int J Electr Power Energy Syst*. 2014;63:760–8.

[12] Eristi H. "Fault diagnosis system for series compensated transmission line based on wavelet transform and adaptive neuro-fuzzy inference system". *Measurement*. 2013;46(1):393–401.

[13] Livani H, Evrenosoglu CY. "A Machine Learning and Wavelet-Based Fault Location Method for Hybrid Transmission Lines". *Smart Grid, IEEE Trans*. 2014;5(1):51–9.